J Plant Res (2013) 126:233–241
DOI 10.1007/s10265-012-0522-6

REGULAR PAPER

Structure and immunocytochemical localization of photosynthetic enzymes in the lamina joint and sheath pulvinus of the C_4 grass *Arundinella hirta*

Masataka Wakayama · Jun-ichi Ohnishi · Osamu Ueno

Received: 21 June 2012 / Accepted: 5 September 2012 / Published online: 17 October 2012

Abstract The C_4 grass *Arundinella hirta* exhibits a unique C_4 anatomy, with isolated Kranz cells (distinctive cells) and C_4-type expression of photosynthetic enzymes in the leaf sheath and stem as well as in the leaf blade. The border zones between these organs are pale green. Those between the leaf blade and sheath and between the sheath and stem are called the lamina joint and sheath pulvinus, respectively, and are involved in gravity sensing. We investigated the structure and localization of C_3 and C_4 photosynthetic enzymes in these tissues. In both zones the epidermis lacked stomata. The inner tissue was composed of parenchyma cells and vascular bundles. The parenchyma cells were densely packed with small intercellular spaces and contained granal chloroplasts with large starch grains. No C_4-type cellular differentiation was recognized. Western blot analysis showed that the lamina joint and pulvinus accumulated substantial amounts of phospho*enol*pyruvate carboxylase (PEPC), pyruvate,Pi dikinase (PPDK), and ribulose 1,5-bisphosphate carboxylase/oxygenase (rubisco). Immunogold electron microscopy revealed PEPC in the cytosol and both PPDK and rubisco in the chloroplasts of parenchyma cells, suggesting the occurrence of C_3 and C_4 enzymes within a single type of chlorenchyma cell. These data indicate that the lamina joint and pulvinus have unique expression patterns of C_3 and C_4 enzymes, unlike those in C_4-type anatomy.

Keywords *Arundinella hirta* · C_4 photosynthesis · Cellular localization of enzymes · C_3 and C_4 photosynthetic enzymes · Lamina joint · Pulvinus

M. Wakayama (✉)
Graduate School of Agricultural and Life Sciences, The University of Tokyo, 1-1-1 Yayoi, Bunkyo-ku, Tokyo 113-8657, Japan
e-mail: amwakaym@mail.ecc.u-tokyo.ac.jp

J. Ohnishi
Division of Life Science, Graduate School of Science and Engineering, Saitama University, 255 Shimo-Ohkubo, Sakura-ku, Saitama, Saitama 338-8570, Japan

O. Ueno
Department of Bioresource Sciences, Faculty of Agriculture, Kyushu University, Hakozaki, Fukuoka 812-8581, Japan

Introduction

The leaves of C_4 plants generally show Kranz-type anatomy. However, many variants on Kranz-type anatomy have been found in various C_4 families. The leaf blades of several NADP-malic enzyme (ME)-type C_4 grasses, such as *Arundinella hirta*, are known to have unusual bundle sheath cells (BSCs) that lie distant from the veins (so-called distinctive cells: DCs), in addition to the usual Kranz units composed of concentric layers of mesophyll cells (MCs) and BSCs surrounding the vascular bundles (Crookston and Moss 1973; Dengler and Dengler 1990; Dengler et al. 1996; Ueno 1995). In most C_4 leaves photosynthetic enzymes are compartmentalized between the MCs and BSCs: phospho*enol*pyruvate carboxylase (PEPC) and pyruvate,Pi dikinase (PPDK) in the MCs, and C_4-acid decarboxylating enzymes such as NADP-ME and ribulose 1,5-bisphosphate carboxylase/oxygenase (rubisco) in the BSCs (Kanai and Edwards 1999). The DCs accumulate the photosynthetic enzymes as in the BSCs (Reger and Yates 1979; Ueno 1995; Wakayama et al. 2003). The mechanisms regulating the cellular differentiation of C_4 leaves and the cell-specific enzyme expression remain intriguing subjects (Hibberd and Covshoff 2010; Langdale 2011; Nelson 2011; Wang et al. 2011). Previous studies have suggested that veins play a key role in the differentiation of C_4 leaf anatomy and a vein-derived positional signal is essential

for the cell-specific enzyme expression of C_4 plants such as maize (Langdale 2011; Nelson 2011). However, *Arundinella hirta* has the DCs not associated with veins in leaves, and the cell-specific enzyme expression of C_4 plant type occurs between the MCs and DCs (Wakayama et al. 2003). Thus this plant provides a unique opportunity to study these subjects.

In higher plants, the major photosynthetic organ is the leaf, but other organs can also photosynthesize (Aschan and Pfanz 2003). In grasses, the leaf sheath, stem, and spike components contain considerable amounts of chlorophyll. In these organs of *A. hirta*, the MCs, BSCs, and DCs are differentiated as in the leaf blade, although some modification occurs in the cellular configuration and the pattern of expression of photosynthetic enzymes (Wakayama et al. 2006).

Pale green tissues intervene between the grass leaf blade and leaf sheath and between the leaf sheath and stem. These border zones are called the lamina joint and the pulvinus, respectively. Both zones contain chloroplasts with large starch grains, called statoliths, and are responsible for leaf and stem gravistimulation (Kaufman et al. 1987; Maeda 1958, 1961; Nakano and Maeda 1978; Parker 1979; Song et al. 1988). The biochemical and physiological mechanisms of the gravitropic response in the pulvinus have been studied in oat and maize (Chang et al. 2001; Clore et al. 2008; Johannes et al. 2001; Perera et al. 1999). However, it is unknown whether the pale chlorophyll-containing tissues of the lamina joint and pulvinus can photosynthesize. We can ask whether the starch grains in chloroplasts are originated from photosynthetic products generated from atmospheric CO_2 or endogenous respiratory CO_2. It is also interesting to ask whether these tissues show the C_4 anatomical features as in leaf blades and stems and carry out C_4 type of metabolism, if they have photosynthetic function. Tsutsumi et al. (2007) did not find mRNAs for photosynthesis genes (*rbcS* and *cab*) in the lamina joint of C_3 rice by in situ hybridization.

Here, we investigated the structural features and cellular localization of C_3 and C_4 photosynthetic enzymes in the lamina joint and pulvinus of *A. hirta*. We selected *A. hirta* because the structural and functional features of its leaf blade and other green organs have been thoroughly studied (Wakayama et al. 2003, 2006). Our main aim was to investigate whether cellular differentiation occurs in the chlorophyll-containing tissues of the lamina joint and sheath pulvinus, as in the leaf blade.

Materials and methods

Plant material

Plants of *Arundinella hirta* (Thunb.) C. Tanaka were collected in the field in Saitama City, Japan, and were propagated from tillers (Wakayama et al. 2003, 2006). Plants were grown in potted, sufficiently fertilized field soil in a growth chamber with a light–dark cycle of 14 h at 25 °C and 10 h at 20 °C. Artificial illumination was provided by metal-halide lamps at a photosynthetic photon flux density 300 μmol m^{-2} s^{-1} (wavelength 400–700 nm) at examined leaves. Samples were taken at 2 to 3 months, when the flag leaves were fully expanded and the flowers were open. All samples were collected from exposed parts of the same phytomer. For experiments, the leaves just below the flag leaves were examined. Leaves were carefully divided into blades, lamina joints, leaf sheaths, and sheath pulvini (Figs. 1a, b, 2a–c). Stems just below the leaves were also examined. The features of the pulvinus differ among grass phylogenetic groups: the festucoid grasses have only a sheath pulvinus, whereas the panicoid grasses, including *A. hirta*, have both a sheath pulvinus and a stem pulvinus (Fig. 2b, c) (Dayanandan et al. 1977). We investigated only the sheath pulvinus, because the stem pulvinus is tightly surrounded by the sheath pulvinus and its photosynthetic function would be much lower. All samples were collected 1.5 h after the start of the light period.

Fig. 1 Structures of the lamina joint and adjacent regions of *Arundinella hirta*. **a** Overview. **b** Locations of photographs. **c**, **e**, **g**, **i** Paradermal views. **d**, **f**, **h**, **j**–**m** Transverse sections. **c**, **d** Leaf blade. **e**, **f** Lamina joint. **g**, **h** Transitional area between lamina joint and leaf sheath. **i**, **j** Leaf sheath. **k** Lamina joint area near leaf blade. **l** Lamina joint area near ligule. **m** Lamina joint area near leaf sheath. *Bar* for **a** = 5 mm, *bars* for **c**–**m** 50 μm. *BSC* bundle sheath cell, *CO* collenchyma, *DC* distinctive cell, *LB* leaf blade, *LG* ligule, *LJ* lamina joint, *LS* leaf sheath, *MC* mesophyll cell, *SC* sclerenchyma, *SO* stoma, *ST* stem, *TR* trichome, *V* vascular bundle

Light- and electron-microscopic observations

Samples were fixed with 3 % glutaraldehyde in 50 mM sodium phosphate buffer (pH 6.8) at room temperature for 3 h, and then washed in phosphate buffer. Washed samples were post-fixed in 2 % OsO_4 in the same buffer, dehydrated through a graded acetone series, and embedded in Spurr's resin as described by Wakayama et al. (2003). Ultrathin sections on copper grids were stained with lead citrate and observed under a transmission electron-microscope (model H-7000, Hitachi, Japan). Semithin sections (about 1 μm thick) on glass slides were stained with toluidine blue O and observed under a light microscope (Nikon Biophot, Tokyo, Japan).

Samples fixed with 3 % glutaraldehyde were also hand-sectioned with a razor blade. Sections on a glass slide were observed by mounting in water under the light microscope for the cellular distribution of chloroplasts.

Antisera

Antisera raised against PEPC and PPDK from maize leaves were generously provided by Drs. T. Sugiyama

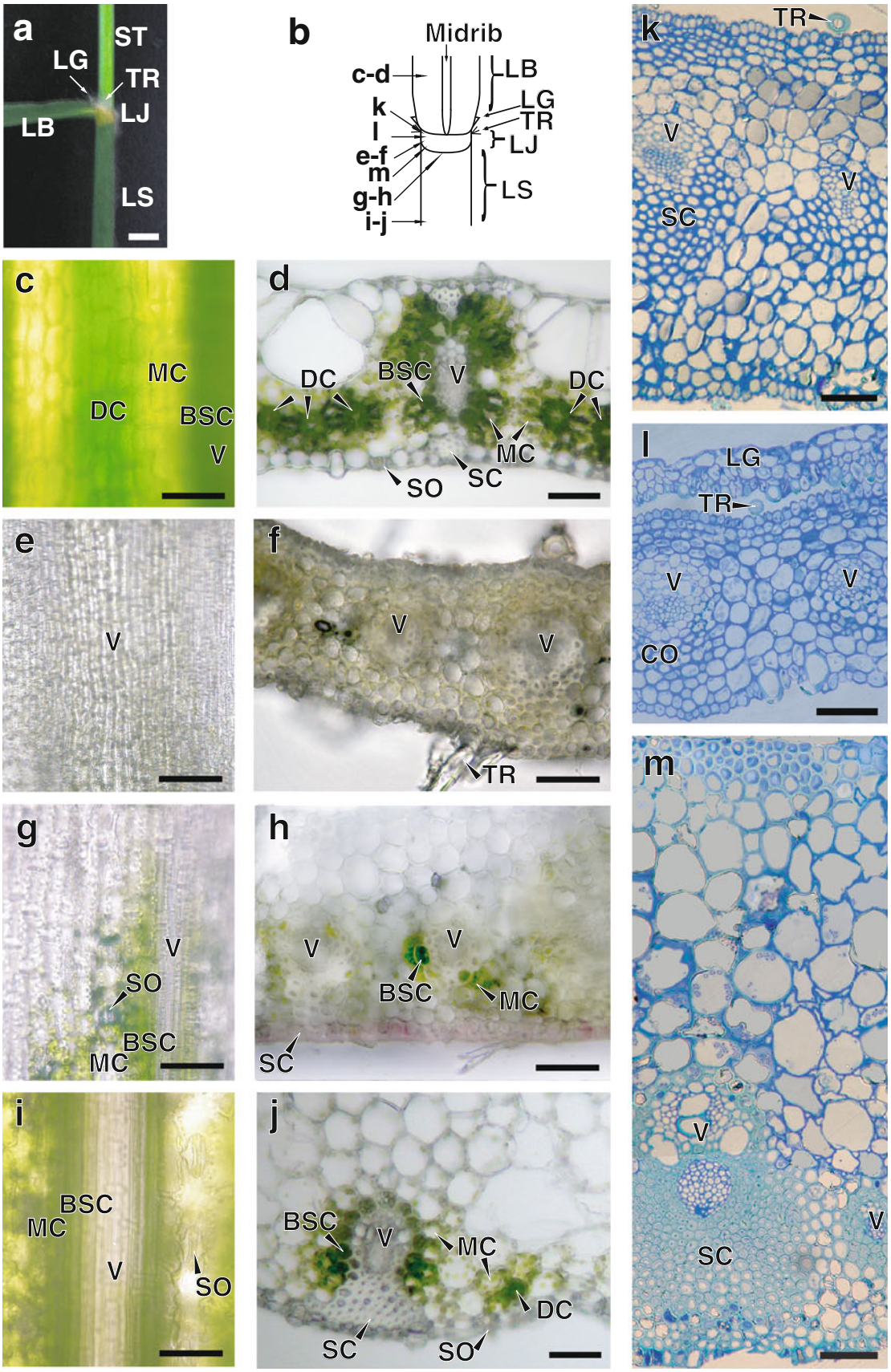
a
ST
LG
TR
LJ
LB
LS
b
Midrib
c-d
LB
LG
k
TR
l
LJ
e-f
m
LS
g-h
i-j
k
TR
V
V
SC
c
MC
DC
BSC
V
d
DC
BSC
V
DC
MC
SO
SC
l
LG
TR
V
V
CO
e
V
f
V
V
TR
m
V
V
SC
g
V
SO
BSC
MC
h
V
V
BSC
MC
SC
i
BSC
MC
V
SO
j
BSC
V
MC
DC
SC
SO

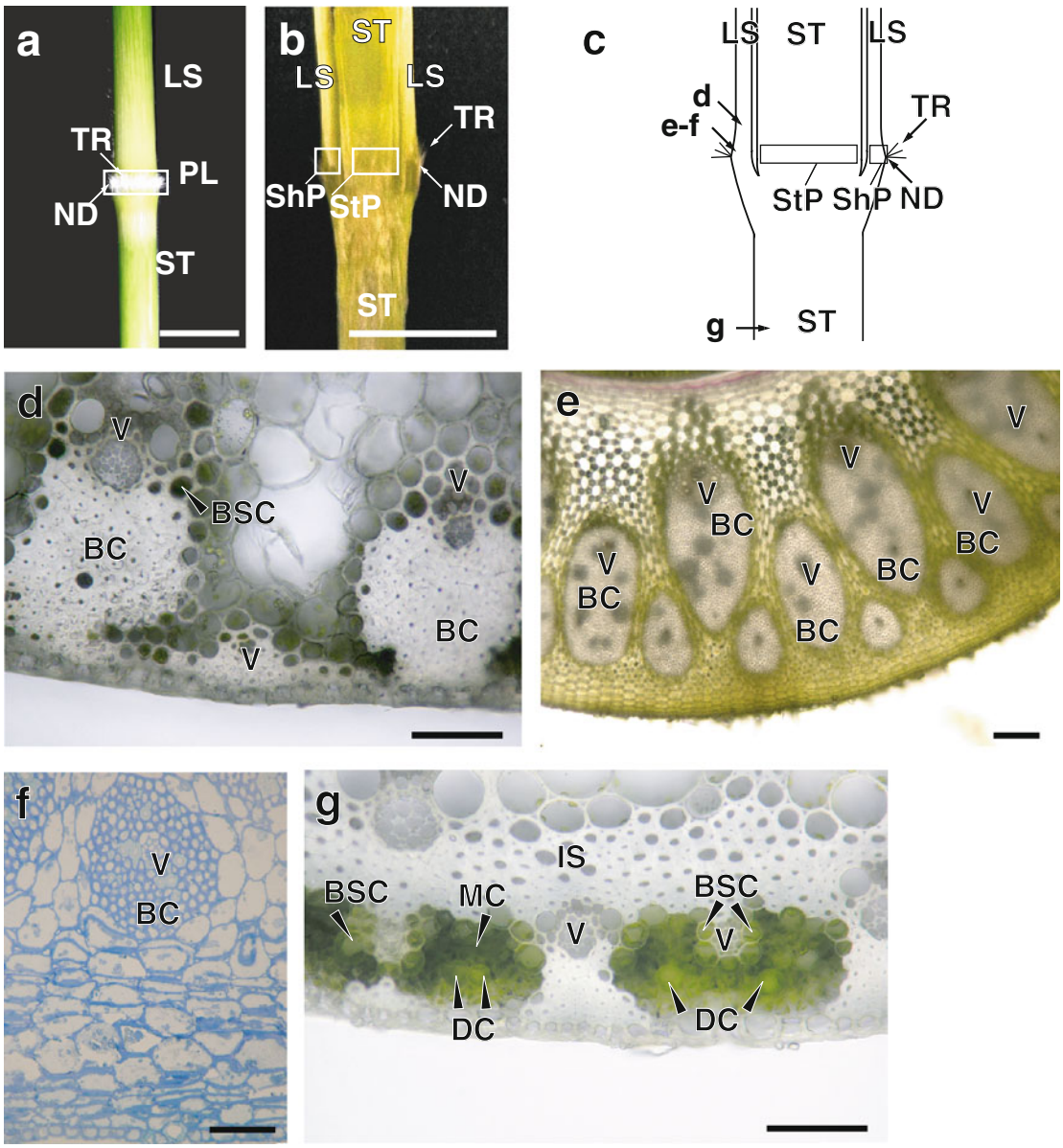

Fig. 2 Structures of the sheath pulvinus and adjacent regions of *Arundinella hirta*. **a** Overview. **b** Longitudinally cut view. **c** Locations of photographs. **d** Transitional area between leaf sheath and sheath pulvinus. **e, f** Sheath pulvinus just above the node. **g** Stem. Bars for **a** and **b** = 5 mm, Bars for **d**–**g** = 50 μm. *BC* bundle cap, *IS* inner sclerenchyma, *LS* leaf sheath, *ShP* sheath pulvinus, *ND* node, *PL* pulvinus, *StP* stem pulvinus. Other abbreviations as in legend to Fig. 1

and H. Sakakibara (RIKEN, Yokohama, Japan). Antiserum against the large subunit (LS) of rubisco from pea leaves was a kind gift of the late Dr. S. Muto (Nagoya University, Nagoya, Japan). These antisera were the same as those used in our previous studies on *A. hirta* (Wakayama et al. 2003, 2006). In these studies, it was confirmed that the antisera specifically recognized PEPC, PPDK, and rubisco LS in the leaf blade, leaf sheath, stem, and spike components of *A. hirta*.

Western blots

The lamina joints and pulvini were collected from about 40 plants and stored in a deep freezer (−80 °C) until homogenization. Samples of lamina joints (0.8 g fresh weight) and pulvini (0.6 g fresh weight) were ground with a pestle in a mortar (on ice) using 1 mL grinding medium, 25 mg polyvinylpyrrolidone and 0.5 g sea sand. The grinding medium contained 50 mM HEPES–KOH (pH 7.5), 0.2 mM EDTA, 5 mM DTT, 0.2 % (v/v) Triton X-100, 1 mM

phenylmethylsulfonyl fluoride, and 0.1 mM leupeptin. Homogenates were filtered through single layer of gauze, and the filtrates were centrifuged at 10,000×*g* for 5 min at 4 °C. Leaf blades (0.25 g fresh weight) were also ground as described above to compare with the lamina joints and pulvini. The supernatants were tested by SDS-PAGE and western blotting as described by Wakayama et al. (2006).

Immunogold electron microscopy

Samples from three plants were fixed with 3 % paraformaldehyde and 0.2 % glutaraldehyde in 50 mM sodium phosphate buffer (pH 6.8) for 3 h on ice. They were washed in phosphate buffer, dehydrated through an ethanol series, and embedded in Lowicryl K4M resin (Chemische Werke Lowi GmbH, Waldkraiburg, Germany) at −20 °C, as described by Wakayama et al. (2003, 2006). Ultrathin sections were collected on 100-mesh nickel grids coated with formvar. The sections on grids were incubated in 0.5 % (W/V) bovine serum albumin (BSA) in phosphate buffered saline (PBS) containing 10 mM sodium phosphate (pH 7.2), 150 mM NaCl and 0.1 % (v/v) Tween 20 for 20 min and then in antiserum diluted with 0.5 % BSA in PBS. The antisera were used at dilution of 1:500 for PEPC and PPDK and at 1:1,000 for the LS of rubisco. For negative controls, antiserum was replaced with non-immune serum. The grids were washed several times with PBS and incubated in a 1:40 dilution of a suspension of 15-nm protein A-colloidal gold (E.Y. Lab. Inc., San Mateo, CA, USA) for 30 min. After several washes with PBS and distilled water, the sections were stained with lead citrate.

Quantitative analysis of immunogold particle density

The labeling density of immunogold particles for photosynthetic enzyme proteins was measured using sections from a lamina joint and a sheath pulvinus of a representative plant. The immunogold particles were counted on electron micrographs at 20,000× magnification, and their labelling density was calculated as the number per unit area (μm^2) by analysing electron micrographs scanned at 400 dpi on a computer with the NIH Image program (US National Institutes of Health). For profiles of chloroplasts, the area occupied by starch grains was excluded. Six or more individual cells were examined in several immunogold-labelled sections for each tissue.

Results

Structural features of the lamina joint

The lamina joint spanned about 3 mm between the leaf blade and leaf sheath and contained less chlorophyll than either (Fig. 1a, b). At its upper portion, the surface was covered by trichomes. Ligules were present in its margins.

The leaf blade had two types of Kranz cells (BSCs and DCs) surrounded by MCs (Fig. 1c, d), as reported (Wakayama et al. 2003). Differentiation of these photosynthetic cells was also observed in the leaf sheath (Fig. 1i, j) and the stem (Fig. 2g) (Wakayama et al. 2006). The lamina joint had no stomata on either surface (Fig. 1e). The inner tissues were composed of parenchyma cells and vascular bundles. The parenchyma cells were structurally uniform (Fig. 1f, k–m), unlike in the leaf blade (Fig. 1d), leaf sheath (Fig. 1j) and stem (Fig. 2g). Thus, no differentiation of the MCs, BSCs and DCs was recognized in the lamina joint, although several BSCs occurred outside vascular bundles in the transitional zones between the lamina joint and leaf blade (data not shown) and between the lamina joint and leaf sheath (Fig. 1g, h). The parenchyma cells were spherical and densely packed and had only small intercellular spaces (Fig. 1f, k–m). These cells contained chloroplasts, but fewer than in the MCs of the leaf blade and leaf sheath (Fig. 3a). The chloroplasts had well developed grana and contained large starch grains (Fig. 3b). However, the chloroplasts were scattered within each cell without uniform orientation (Fig. 1l, m). The vascular bundle was surrounded partly by thick-walled cells (Fig. 1f, m). The phloem side of the vascular bundles was girdled with collenchyma in the zone near the ligule (Fig. 1l) and with sclerenchyma in the other zones (Fig. 1k, m).

Structural features of the sheath pulvinus

The sheath pulvinus spanned about 5 mm between the leaf sheath and stem and contained a small amount of chlorophyll (Fig. 2a–c). The surface was covered by trichomes. The node was present in the middle part of sheath pulvinus (Fig. 2b, c). No stomata were observed on either surface (Fig. 2e).

The inner tissues were composed of parenchyma cells and vascular bundles girdled by large round sclerenchyma (Fig. 2e, f), called the bundle cap in previous studies (Paiva and Machado 2003; Parker 1979). The parenchyma cells were densely packed and had only small intercellular spaces (Fig. 2e, f). Those near the epidermis showed a pressed shape (Fig. 2e, f). No differentiation of the MCs, BSCs and DCs was observed. The parenchyma cells contained fewer chloroplasts than the leaf sheath and stem. The chloroplasts had grana and large starch grains (Fig. 3c, d). In the transitional zone between the sheath pulvinus and the leaf sheath, the bundle caps were reduced, and the chlorophyll content was increased with the development of small BSCs (Fig. 2d). Below the node area, the bundle caps were gradually diminished, and the structural features changed gradually to those in the stem (Fig. 2g).

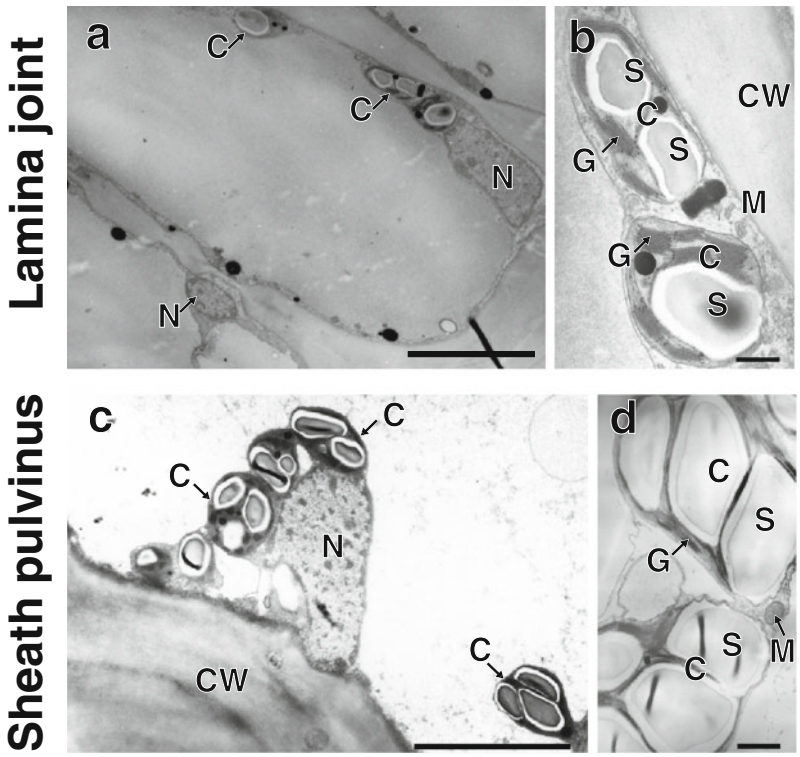

Fig. 3 Ultrastructure of the lamina joint (**a**, **b**) and sheath pulvinus (**c**, **d**) of *A. hirta*. **a** Parenchyma cells of lamina joint. **b** Chloroplasts of a parenchyma cell. **c**, **d** Chloroplasts of parenchyma cells of sheath pulvinus. *Bars* for **a** and **c** = 5 μm, *bars* for **b** and **d** = 0.5 μm. *C* chloroplast, *CW* cell wall, *G* grana, *S* starch grain, *M* mitochondrion, *N* nucleus

Western blot analysis of C_3 and C_4 photosynthetic enzymes

The leaf blade accumulated substantial amounts of the enzymes involved in the C_3 and C_4 pathways, namely, rubisco LS, PEPC and PPDK (Fig. 4). Both the lamina joint and pulvinus also accumulated these enzymes, but in lesser amounts (Fig. 4).

Immunogold localization of C_3 and C_4 photosynthetic enzymes

The cellular localization of C_3 and C_4 photosynthetic enzymes was examined in the parenchyma cells of the lamina joint and sheath pulvinus (Fig. 5). When sections of the lamina joint and sheath pulvinus were incubated in control non-immune serum, they showed evidence of only non-specific and negligible labelling with colloidal gold (Fig. 5a, e). Gold particles labelling PEPC and PPDK were observed in the cytosol (Fig. 5b, f; Table 1) and chloroplasts (Fig. 5c, g; Table 1), respectively. Gold particles labelling rubisco LS were observed in the chloroplasts (Fig. 5d, h; Table 1). Such labelling patterns of immunogold particles were uniformly found in all parenchyma cells of the lamina joint and sheath pulvinus. Therefore, it appeared that the C_3 and C_4 enzymes occurred within the same parenchyma cell without indication of intercellular compartmentalization.

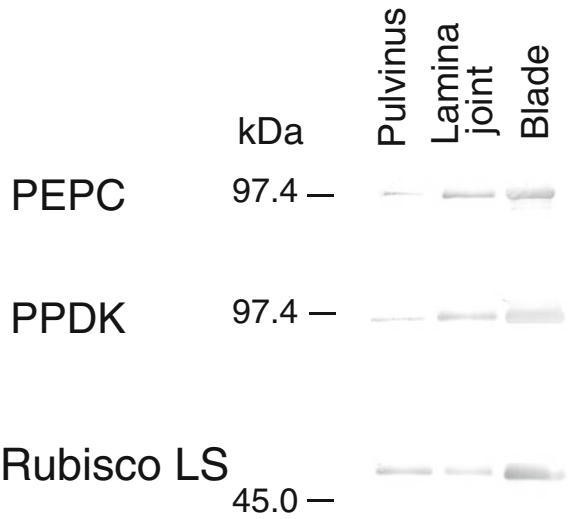

Fig. 4 Western blots of proteins extracted from the pulvinus, lamina joint and leaf blade of *A. hirta*. Total soluble protein (5 μg for PEPC and PPDK; 1 μg for rubisco LS) was subjected to SDS-PAGE, blotted on nitrocellulose membranes, and identified with antisera

Discussion

Our results (Figs. 1, 2, 3) show that the MCs, BSCs and DCs are not differentiated in the lamina joint and sheath pulvinus of *A. hirta*. Instead, the parenchyma is composed of uniform cells with chloroplasts, which accumulate many large starch grains and developed granal thylakoids. These

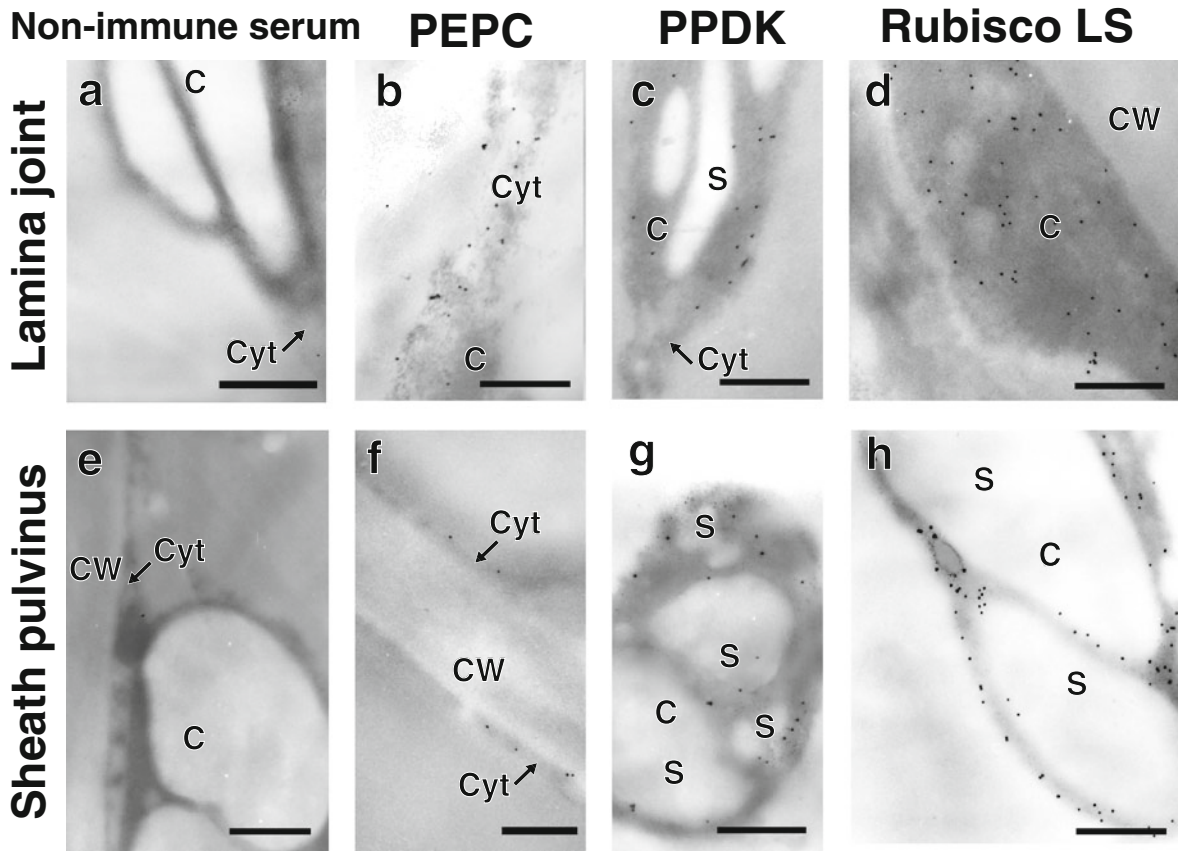

Fig. 5 Immunogold localization of photosynthetic enzymes in abaxial parenchyma cells of (**a**–**d**) lamina joint near ligule and (**e**–**h**) sheath pulvinus just above the node of *A. hirta*. **a**, **e** Non-immune serum. **b**, **f** PEPC. **c**, **g** PPDK. **d**, **h** Rubisco LS. Bars = 0.5 μm. *Cyt* cytosol. Other abbreviations as in legends to Fig. 3

Table 1 Densities of immunogold labeling of photosynthetic enzymes in the parenchyma cells of the lamina joint and sheath pulvinus of *A. hirta*

Organ	Organelle	Density of labeling (counts μm^{-2})		
		PEPC	PPDK	Rubisco LS
Lamina joint	Chloroplast	–	26.6 ± 2.8 (19)	39.2 ± 6.6 (13)
	Cytosol	16.5 ± 8.1 (16)	–	–
	Other	0.4 ± 0.1 (9)	ND (9)	0.2 ± 0.1 (9)
Sheath pulvinus	Chloroplast	–	15.4 ± 0.5 (13)	75.6 ± 1.2 (12)
	Cytosol	14.0 ± 0.9 (9)	–	–
	Other	0.4 ± 0.1 (15)	0.6 ± 0.4 (8)	ND (9)

Densities of immunogold labelings were given as mean ± SE. Numbers in parentheses show the numbers of organelles examined. The labeling densities of other organelles for PEPC include those of chloroplasts. The labeling densities of other organelles for PPDK and Rubisco LS include those of cytosol

ND not detectable

structural features together with the data of photosynthetic enzyme accumulation (Fig. 4) suggest that the chloroplasts are photosynthetically functional. In the context of the photosynthetic function of the chlorenchyma, it is important to note that both the adaxial and abaxial epidermis lack stomata. This fact indicates that atmospheric CO_2 is not directly diffused into the chlorenchyma of the lamina joint and sheath pulvinus. Instead, it may enter via intercellular spaces from the adjacent tissues—the leaf blade, leaf sheath and stem—in which stomata are present. However, the chlorenchyma cells of the lamina joint and sheath pulvinus were compacted, and the intercellular spaces were much smaller than those in the MCs of the leaf blade, leaf sheath and stem. As a result, the supply of CO_2 from such

pathways would be restricted. Thus, it seems that respiratory CO_2 is a carbon source for photosynthesis in the chlorenchyma cells. However, it cannot be ruled out that sugar transported from other photosynthetic tissues adjacent to the lamina joint and sheath pulvinus may be also responsible for the starch grains accumulated in chloroplasts.

Western blot analysis (Fig. 4) showed that the lamina joint and pulvinus also accumulated PEPC, PPDK and rubisco LS proteins, although less than in the leaf blade. Our preliminary study showed that the lamina joint and pulvinus had substantial activities of PEPC, NADP-ME and rubisco but the activities were lower than those in the leaf blade, leaf sheath and stem (unpublished data). The immunogold localization study identified PEPC in the cytosol and PPDK and rubisco in the chloroplasts of the chlorenchyma cells. Although more rigorous examination, such as a double labelling study of PEPC and rubisco on the same section (Bendayan 2000) and/or an immunohistochemical study of larger scale on serial sections obtained from the same sample (e.g., Voznesenskaya et al. 2005), will be required, it appears that the C_3 and C_4 photosynthetic enzymes occur within the single-type chlorenchyma cells of the lamina joint and sheath pulvinus of *A. hirta*. This cellular localization pattern differs from that in the leaf blade of C_4 plants, including *A. hirta*, in which cytosolic PEPC and chloroplastic PPDK are localized in the MCs, and chloroplastic rubisco in the BSCs (Kanai and Edwards 1999; Wakayama et al. 2003).

This pattern of intracellular localization of the C_3 and C_4 photosynthetic enzymes recognized in the lamina joint and sheath pulvinus of *A. hirta* differ from that found in C_4 chenopods, in which the enzymes are compartmentalized between organelles within a single cell together with structural specialization of organelles, essentially replicating the compartmentalization between the two cell types in typical C_4 plants (Voznesenskaya et al. 2001; 2002). We did not confirm the intracellular localization of C_4-acid decarboxylating enzymes such as NADP-ME. In addition, it remains unknown whether the PEPC found in the lamina joint and sheath pulvinus is a C_4 specific form. Nevertheless, the intracellular localization pattern of PEPC, PPDK and rubisco in the lamina joint and pulvinus are reminiscent of those found in *Hydrilla verticillata*, in which a C_4-like metabolism with decarboxylation by chloroplastic NADP-ME operates within a single photosynthetic cell (Bowes 2011; Reiskind et al. 1989). In crassulacean acid metabolism (CAM) plants also, both C_3 and C_4 photosynthetic enzymes coexist within a single mesophyll cell, although the activation and inactivation of PEPC are regulated diurnally (Kondo et al. 1998; Winter and Smith 1996). It seems that the levels of photosynthetic activity in the lamina joint and sheath pulvinus are much lower than that in the leaf blade. Recently, it has been posited that the stem chlorenchyma of some trees also performs C_4-like metabolism with high PEPC activity (Pfanz et al. 2002). However, Berveiller et al. (2007) suggested that PEPC in tree stems plays a role in non-photosynthetic carbon fixation, such as of respired CO_2 and via the anaplerotic pathway. It is also known that guard cells of the stoma contain both C_3 and C_4 photosynthetic enzymes (Parvathi and Raghavendra 1997; Ueno 2001). Although further investigation is needed to elucidate the exact carbon metabolism(s) functioning in the chlorenchyma of the lamina joint and sheath pulvinus, fixation of respiratory CO_2 and release of O_2 by photosynthesis may help to avoid anoxia in the closed tissues without stomata and with very small intercellular spaces.

To prevent the chloroplasts from re-sedimenting we did not maintain the tissue samples in their correct orientation during fixation. Thus, we cannot identify the exact localization of statolith chloroplasts in the lamina joint and pulvinus. Previous studies of pulvini of some grasses reported sedimented statolith chloroplasts in the chlorenchyma cells surrounding the vascular bundles (Chang et al. 2001; Parker 1979). In oat shoot pulvini, the starch level changes as plants are reoriented, and it has been suggested that protein dephosphorylation and calcium mediate starch metabolism in response to a gravistimulation signal (Chang et al. 2001). We found no difference in the cellular localization pattern of the C_3 and C_4 photosynthetic enzymes between the chlorenchyma cells surrounding vascular bundles and other chlorenchyma cells. Thus, it seems that there is no difference in the photosynthetic carbon metabolism between these cells. However, a detailed study of the starch metabolism would be required.

Acknowledgments We thank Dr. T. Sugiyama, Dr. H. Sakakibara and the late Dr. S. Muto for providing the antisera.

References

Aschan G, Pfanz H (2003) Non-foliar photosynthesis—a strategy of additional carbon acquisition. Flora 198:81–97

Bendayan M (2000) A review of the potential and versatility of colloidal gold cytochemical labeling for molecular morphology. Biotech Histochem 75:203–242

Berveiller D, Vidal J, Degrouard J, Ambard-Bretteville F, Pierre J, Jaillard D, Damesin C (2007) Tree stem phospho*enol*pyruvate carboxylase (PEPC): lack of biochemical and localization evidence for a C_4-like photosynthesis system. New Phytol 176:775–781

Bowes G (2011) Single-cell C_4 photosynthesis in aquatic plants. In: Raghavendra AS, Sage RF (eds) C_4 photosynthesis and related CO_2 concentrating mechanism. Springer, Dordrecht, pp 63–80

Chang S-C, Cho MH, Kang BG, Kaufman PB (2001) Changes in the starch content in oat (*Avena sativa*) shoot pulvini during the gravitropic response. J Exp Bot 52:1029–1040

Clore AM, Doore SM, Tinnirello SMN (2008) Increased levels of reactive oxygen species and expression of a cytoplasmic aconitase/iron regulatory protein 1 homolog during the early response of maize pulvini to gravistimulation. Plant Cell Environ 31:144–158

Crookston RK, Moss DN (1973) A variation of C_4 leaf anatomy in *Arundinella hirta* (Gramineae). Plant Physiol 52:397–402

Dayanandan P, Hebard FV, Baldwin VD, Kaufman PB (1977) Structure of gravity-sensitive sheath and internodal pulvini in grass shoots. Amer J Bot 64:1189–1199

Dengler RE, Dengler NG (1990) Leaf vascular architecture in the atypical C_4 NADP-malic enzyme grass *Arundinella hirta*. Can J Bot 68:1208–1221

Dengler NG, Donnelly PM, Dengler RE (1996) Differentiation of bundle sheath, mesophyll, and distinctive cells in the C_4 grass *Arundinella hirta* (Poaceae). Am J Bot 83:1391–1405

Hibberd JM, Covshoff S (2010) The regulation of gene expression required for C_4 photosynthesis. Annu Rev Plant Biol 61:181–207

Johannes E, Collings DA, Rink JC, Allen NS (2001) Cytoplasmic pH dynamics in maize pulvinal cells induced by gravity vector changes. Plant Physiol 127:119–130

Kanai R, Edwards GE (1999) Biochemistry of C_4 photosynthesis. In: Sage RF, Monson RK (eds) C_4 plant biology. Academic Press, San Diego, pp 49–87

Kaufman P, Brock T, Song I, Rho Y, Ghosheh N (1987) How cereal grass shoots perceive and respond to gravity. Am J Bot 74:1446–1457

Kondo A, Nose A, Ueno O (1998) Leaf inner structure and immunogold localization of some key enzymes involved in carbon metabolism in CAM plants. J Exp Bot 49:1953–1961

Langdale LA (2011) C_4 cycles: past, present, and future research on C_4 photosynthesis. Plant Cell 23:3879–3892

Maeda E (1958) The effects of growth regulators on the geotropism of leaf sheath basal region in wheat plant. J Exp Bot 9:343–349

Maeda E (1961) Studies on the mechanism of leaf formation in crop plants. II. Anatomy of the lamina joint in rice plant. Proc Crop Sci Soc Jpn 29:234–239

Nakano H, Maeda E (1978) On starch statolith in the lamina joint of rice plants. Jpn J Crop Sci 47:262–266

Nelson T (2011) Development of leaves in C_4 plants: anatomical features that support C_4 metabolism. In: Raghavendra AS, Sage RF (eds) C_4 photosynthesis and related CO_2 concentrating mechanism. Springer, Dordrecht, pp 147–159

Paiva EAS, Machado SR (2003) Collenchyma in *Panicum maximum* (Poaceae): localisation and possible role. Aust J Bot 51:69–73

Parker M (1979) Morphology and ultrastructure of the gravity-sensitive leaf sheath base of the grass *Echinochloa colonum* L. Planta 145:471–477

Parvathi K, Raghavendra AS (1997) Both rubisco and phosphoenol-pyruvate carboxylase are beneficial for stomatal function in epidermal strips of *Commelina benghalensis*. Plant Sci 124:153–157

Perera IY, Heilmann I, Boss WF (1999) Transient and sustained increases in inositol 1,4,5-trisphosphate precede the differential growth response in gravistimulated pulvini. Proc Natl Acad Sci USA 96:5838–5843

Pfanz H, Aschan G, Langenfeld-Heyser R, Wittmann C, Loose M (2002) Ecology and ecophysiology of tree stems: corticular and wood photosynthesis. Naturwissenschaften 89:147–162

Reger BJ, Yates IE (1979) Distribution of photosynthetic enzymes between mesophyll, specialized parenchyma and bundle sheath cells of *Arundinella hirta*. Plant Physiol 63:209–212

Reiskind JB, Berg RH, Salvucci ME, Bowes G (1989) Immunodold localization of primary carboxylases in leaves of aquatic and a C3–C4 intermediate species. Plant Sci 61:43–52

Song I, Lu CR, Brock TG, Kaufman PB (1988) Do starch statoliths act as the gravisensors in cereal grass pulvini? Plant Physiol 86:1155–1162

Tsutsumi K, Kawasaki M, Taniguchi M, Itani T, Maekawa M, Miyake H (2007) Structural and functional differentiation of bundle sheath and mesophyll cells in the lamina joint of rice compared with that in the corresponding region of the liguleless genotype. Plant Prod Sci 10:346–356

Ueno O (1995) Occurrence of distinctive cells in leaves of C_4 species in *Arthraxon* and *Microstegium* (Andropogoneae–Poaceae) and the structural and immunocytochemical characterization of these cells. Int J Plant Sci 156:270–289

Ueno O (2001) Ultrastructural localization of photosynthetic and photorespiratory enzymes in epidermal, mesophyll, bundle sheath and vascular bundle cells of the C_4 dicot *Amaranthus viridis*. J Exp Bot 52:1003–1013

Voznesenskaya EV, Franceschi VR, Kiirats O, Freitag H, Edwards GE (2001) Kranz anatomy is not essential for terrestrial C_4 plant photosynthesis. Nature 414:543–546

Voznesenskaya EV, Franceschi VR, Kiirats O, Artyusheva EG, Freitag H, Edwards GE (2002) Proof of C_4 photosynthesis without Kranz anatomy in *Bienertia cycloptera* (Chenopodiaceae). Plant J 31:649–662

Voznesenskaya EV, Chuong SDX, Kiirats O, Franceschi VR, Edwards GE (2005) Evidence that C_4 species in genus *Stipagrostis*, family Poaceae, are NADP-malic enzyme subtype with nonclassical type of Kranz anatomy (Stipagrostoid). Plant Sci 168:731–739

Wakayama M, Ueno O, Ohnishi J (2003) Photosynthetic enzyme accumulation during leaf development of *Arundinella hirta*, a C_4 grass having Kranz cells not associated with veins. Plant Cell Physiol 44:1330–1340

Wakayama M, Ohnishi J, Ueno O (2006) Structure and enzyme expression in photosynthetic organs of the atypical C_4 grass *Arundinella hirta*. Planta 223:1243–1255

Wang L, Peterson RB, Brutnell TP (2011) Regulatory mechanisms underlying C_4 photosynthesis. New Phytol 190:9–20

Winter K, Smith J (1996) Crassulacean acid metabolism: current status and perspectives. In: Winter K, Smith J (eds) Crassulacean acid metabolism: biochemistry, ecophysiology and evolution. Springer, Berlin, pp 389–426